

Bird-Area Water-Bodies Dataset (BAWD) and Predictive AI Model for Avian Botulism Outbreak (AVI-BoT)

Narayani Bhatia, Devang Mahesh, Jashandeep Singh, and Manan Suri*

Department of Electrical Engineering, Indian Institute of Technology Delhi, India.

*Corresponding author: Manan Suri (e-mail: manansuri@ee.iitd.ac.in).

Abstract

Avian botulism caused by a bacterium, *Clostridium botulinum*, causes a paralytic disease in birds often leading to high fatality, and is usually diagnosed using molecular techniques. Diagnostic techniques for confirming the outbreak of Avian botulism include: Mouse Bioassay, ELISA, PCR (based on post-mortem), all of which are time-consuming, laborious and require invasive sample collection from affected sites or dead birds. All these in-vitro techniques are non-preventive and their processing time may further contribute to the bacterial growth in the affected regions. In this study, we build a first-ever multi-spectral, remote-sensing imagery based global *Bird-Area Water-bodies Dataset (BAWD)* (i.e. fused satellite images of warm-water lakes/marshy-lands or similar water-body sites that are important for avian fauna) backed by on-ground reporting evidence of outbreaks. In the current version, BAWD consists of multi-spectral satellite images, covering a total ground area of 904 sq.km from two open source satellite projects (Sentinel and Landsat). BAWD consists of 17 topographically diverse global sites spanning across 4 continents, where locations were monitored over a time-span of 3 years (2016-2020). Using BAWD and state-of-the-art deep-learning techniques we propose a first-ever Artificial Intelligence based (AI) model to predict potential outbreak of Avian botulism called AVI-BoT (**A**erosol **V**isible, **I**nfra-red (NIR/SWIR) and **B**ands of **T**hermal). AVI-BoT uses fused multi-spectral satellite images of water-bodies (10-bands) as input to generate a spatial prediction map depicting probability of potential Avian botulism outbreaks. We also train and investigate a simpler (5-band) Causative-Factor model (based on prominent physiological factors reported in literature as conducive for outbreak) to predict Avian botulism. Using AVI-BoT, we achieve a training accuracy of 0.94 and validation accuracy of 0.96 on BAWD, far superior in comparison to our model based on causative factors. For detailed feature-space analysis and explain-ability of the proposed 10-band AVI-BoT model, we further train four additional spectral models on BAWD using: (i) Aerosol, (ii) Visible (3-bands), (iii) IR (3-bands), and (iv) Thermal (3-bands). Further, we analyze using AVI-BoT, two recent and highly complex outbreak case-studies: (i) Sambhar Lake (India, November 2019), and (ii) Klamath National Wildlife Refuge (U.S.A., October 2020). The model is found to closely converge with ground-reporting observations at both these sites with a fine-grain spatio-temporal prediction capability. The proposed technique presents a scale-able, low-cost, non-invasive methodology for continuous monitoring of bird-habitats against botulism outbreaks with the potential of saving valuable fauna lives.

1 Introduction

Avian botulism is a paralytic disease that fatally affects birds. It is caused by a bacterium, *Clostridium botulinum*, which produces a Botulinum neurotoxin, ingestion of which often leads to death in birds (Fig. 1). Botulism spores (resting stage of the bacteria) can persist in the soil and aquatic sediments of water bodies for decades before it enters the food webs of birds. Organisms like- algae, plants and invertebrates act as biotic reservoir for the disease and further fishes are known carriers of botulism spores¹. Once the spores enter the food webs of birds, avian botulism spreads in a self-perpetuating manner via the maggot cycle. Maggots which feed on the dead birds, acquire the bacteria and are likely to be eaten by carnivorous birds. The carnivorous birds that die because of the bacteria present in maggots are then fed by other maggots and this way, the cycle continues. Avian botulism is prevalent all over the world, with higher prevalence over North American wetlands. In the previous century the disease has caused an estimated average death of about 644,000 birds per reported outbreak year in U.S.A. and Canada² alone. Some physiological conditions for the bacterium to develop are: low-oxygen, eutrophic

zones, higher water temperatures, shallow stagnant water³. Such non-exhaustive list of causative factors leading to Avian botulism outbreak is one of the key areas of current research⁴. Some of the recent outbreaks in England (2018), Wales (2018)³, Klamath National Wildlife Refuge (2020)⁵ resulted in bird casualty as high as 40,000.

Some of the widely known techniques to confirm the outbreak of Avian botulism are culture techniques⁶, assay test for presence of toxin⁷, PCR test⁸ (See Table 1). Most of these techniques rely on actual ground level sample collection which is challenging due to the requirement of physical access. Further, all the aforementioned techniques are usually used as post-mortem tests⁹, that is, used for detection of conditions only after clinical symptoms or deaths start getting reported from the location. Moreover, in some cases, post-mortem tests may be inconclusive and need to be backed by further laboratory confirmation which adds to the delay⁹. This often leads governments and conservationists with little time for quick relief operations to save precious and endangered fauna.

In order to overcome some limitations of the aforementioned clinical diagnostic methods, we present in this study a first-ever *Bird-Area Water-Bodies Dataset (BAWD)* (i.e. fused satellite images of warm-water lakes/marshy-land etc or similar water-body sites that are important for avian fauna) built from publicly available open-source satellite imagery. Our hand-annotated dataset consists of multi-spectral satellite images, covering a total ground area of 904 sq. km, from two open source satellite projects (Sentinel and Landsat), covering 17 topographically diverse global bird-area water bodies from 4 continents, where locations are monitored over a time-span of 3 years (2016-2020). BAWD includes complete mapping between location scenes and ground-truth labels, backed by reporting of outbreaks. Further, we propose a multi-spectral remote sensing AI detection model called AVI-BoT (**A**erosol **V**isible **I**nfra-red (both NIR and SWIR) - **B**ands of **T**hermal) to predict potential outbreak of Avian botulism. AVI-BoT takes fused multi-spectral satellite images as an input and generates a spatial prediction map depicting probability of an outbreak to occur. Satellite images in BAWD are composed of 10 remote sensing bands which capture the physio-chemical botulinum-promoting parameters such as pH, salinity, temperature among many others. We also train and investigate a simpler (5-band) Causative-Factor model (based on prominent physiological factors reported in literature as conducive for outbreak) to predict Avian botulism outbreak. Notably, AVI-BoT trained as a deep convolution neural network over BAWD, achieves far superior performance with a validation accuracy of 0.96. Further, two recent and highly complex Avian botulism outbreaks namely at Sambhar Lake (India, November 2019)¹² and Klamath National Wildlife Refuge (U.S.A., October 2020)⁵ are investigated using AVI-BoT. At both the locations, AVI-BoT provides excellent forecasting of both severity and spatial distribution of the outbreak, validated using field reporting. We then use the model on satellite data collected from these locations over a time-span of 3 years and 1 year respectively to investigate the formation of Avian botulism conducive conditions which exacerbated and resulted in mass die-offs. To take a closer look at the evolution of the feature representations learnt by AVI-BoT, we additionally train four direct spectral models: ((i) Aerosol, (ii) Visible (3-bands), (iii) IR (3-bands), and (iv) Thermal (3-bands)).

The proposed work combines recent advances in the domains of deep learning and multi-spectral remote sensing. It provides a fast, scalable, non-invasive, first-of-a-kind monitoring and predictive methodology for avian life conservation. The model is made sufficiently generic by covering 17 locations across 4 continents, as well as covering a range of physical, chemical, biological factors responsible for the outbreak to occur.



Figure 1: (a) Bacterium - Clostridium botulinum¹⁰, (b) Healthy bird¹¹, (c) Affected bird suffering from paralysis of neck muscles due to Avian botulism².

Table 1: State of the Art techniques for detection of Avian botulism.

Paper	Objective of Study	Locations Covered	Underlying Methodology	Key Contribution
13	Detection	2 locations	Mouse BioAssay (Clinical, Bio-chemical)	Identification of the neurotoxin produced by Clostridium botulinum using mouse bioassay technique
7;14	Detection	-	ELISA (Clinical, Bio-chemical)	Identification of the neurotoxin produced by Clostridium botulinum using microplates
8	Detection	-	PCR (Clinical, Bio-chemical)	Reviews PCR-based assay along with primers, sensitivity
15	Detection	-	Pre-PCR (Clinical, Bio-chemical)	Optimized pre-PCR processing by proposing the use of liver
This work	Detection, Prediction of potential outbreaks	17 locations 4 continents	Salinity, Temperature, pH, Organic Matter (Remote sensing AI-based Computational-Deep Learning Network)	Proposed use of AVI-BoT Model using temporal multispectral remote sensing data of 10-100m resolution from Sentinel 2 and Landsat 8

2 Results

2.1 AI Model Bench-marking

Fig. 2 shows the accuracy and loss plots for training and validation for the two proposed models: (i) Causative Factors based model (5-bands) and (ii) AVI-BoT model (10-bands). (For all details on model training, pipeline and methodology refer to (Methods) Section 5.) The Causative factors model based on factors inspired from literature shows inferior training and validation accuracy compared to AVI-BoT model, thereby necessitating the inclusion of multiple diverse spectral features (detailed in Table 5). The 10-band AVI-BoT model (which is a combination of aerosol, visible-spectra, NIR-SWIR, and thermal bands) capably combines all hypothesized factors in the feature representation and achieves a training accuracy of 0.94 and a validation accuracy of 0.96.

2.2 Outbreak Case-Studies

To test the capability of the proposed AVI-BoT model, we analyzed two locations with recently reported complex cases of Avian botulism outbreak. The complexity of these two locations arise from the dynamic and evolving on-ground situation, unexpectedly worsening within a matter of days, affecting a large number of birds before authorities could take action. It is noteworthy that in both these cases, none of the on-ground apparatus had reported even an inclination towards an impending outbreak. These test case-studies include:

- Sambhar Lake, Rajasthan, India in November 2019¹².
- Klamath National Wildlife Refuge, California, USA in October 2020⁵.

2.2.1 Case Study 1: Sambhar Lake

Sambhar Lake (India) had witnessed an outbreak in November 2019¹². In Fig. 3 (g) Causative factors based model shows the result as ‘no outbreak’, which is a wrong prediction w.r.t reported ground-truth. Whereas in Fig. 3 (h), the AVI-BoT model gives an accurate picture by capturing the severity as well as the spatial extent of the outbreak. Delving deeper into the AVI-BoT prediction, we perform a comparison

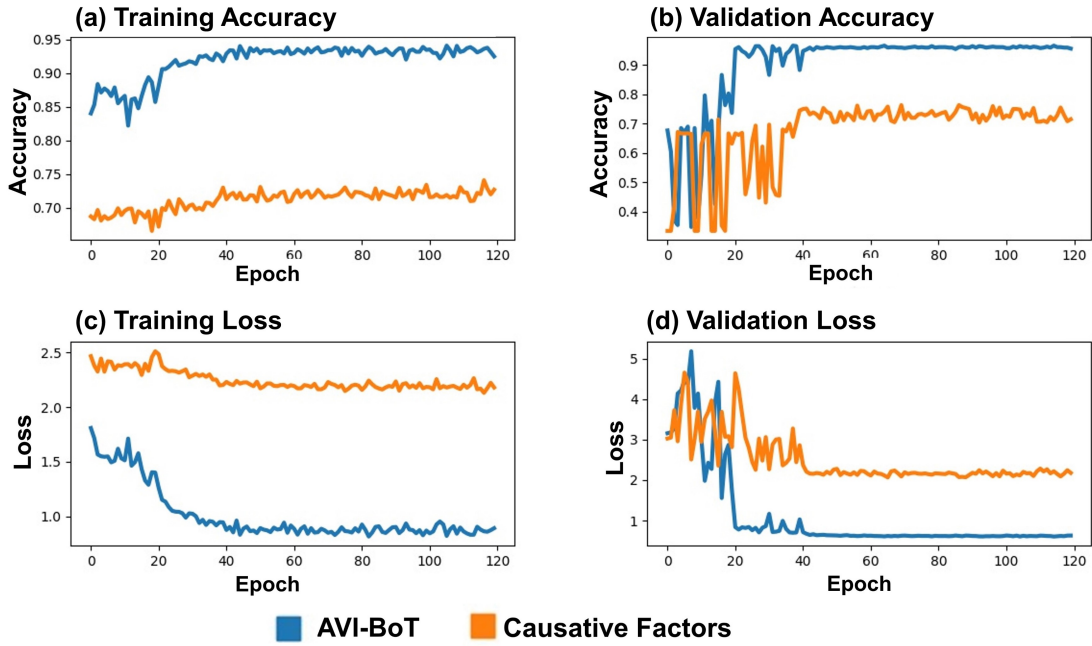
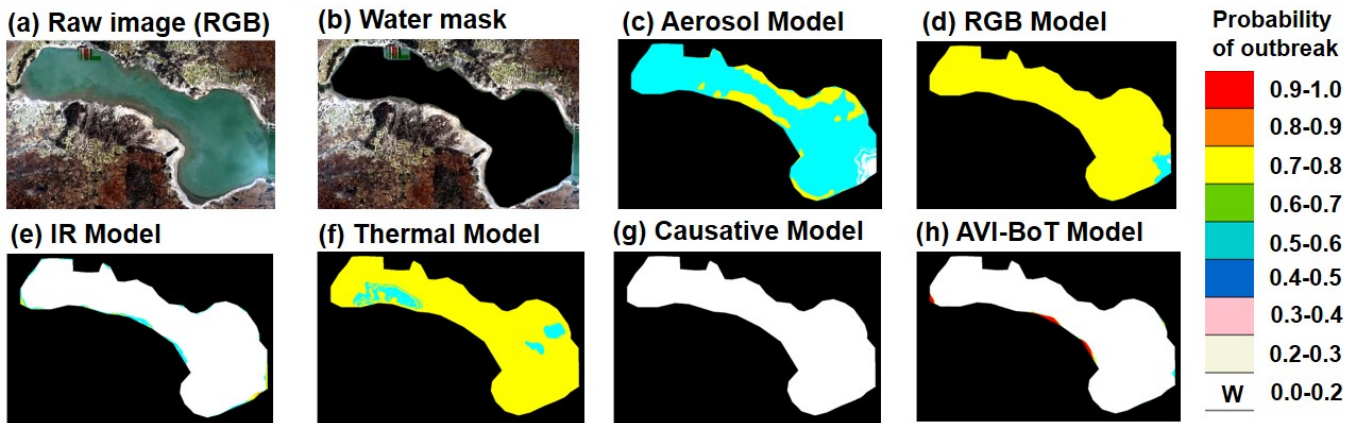


Figure 2: Epoch-wise scores for proposed Causative Factors and AVI-BoT models: (a) Training Accuracy, (b) Validation Accuracy, (c) Training Loss, and (d) Validation Loss.

with the actual on-ground reporting of the outbreak¹⁶. Fig. 4 (a) shows the prediction by AVI-BoT model on the sample dated 19th November 2019, which shows a red prediction (probability of outbreak > 0.9) on two locations - top left which corresponds to Nagaur district, and left shoreline which corresponds to Jaipur district. Fig. 4 (b) shows the district-wise map of Sambhar Lake along with reported carcass count for the two affected districts - Nagaur and Jaipur, for an overlapping 9 day period. Clearly from Fig. 4, AVI-BoT model is able to predict two locations of the outbreak and the severity, accurately. For further analysis, we present a temporal prediction map for the susceptible months during a three year span of 2017-2019, analyzing the trends of outbreak probabilities (Table 2). Key observations are:

1. September 2017 (Table 2 (a)) is marked by a strong deficiency in rainfall which exacerbate conditions near the neck of the river. However, the decrease in water level is so high that the left part of the lake almost disappears (Table 2 (b)), hence moderate conditions appear near the top of the right part of the lake.
2. Higher prediction observed at the edges of the lake, instead of the center, which are also the preferred habitat of the migratory birds. The neck of the lake (corresponding to an on-ground distance of 2 km) is the main dead-point where conditions are most strong. (Table 2 (e))
3. The year 2018 shows the build-up of conditions steadily over time. Further, increased evaporation has led to sharp recession of water-levels, thereby exposing the ground below. Higher evaporation can be interpreted as warmer water temperatures, which is one of the breeding grounds for the bacterium. (Table 2 (c)-(g))
4. 2019 again shows a steady progression over time and spread from the lower right end of the lake towards the left edge. (Table 2 (h)-(n))
5. The analysis shows that for the same month, situation might change drastically from year to year. Example, September month of 2017, 2018 and 2019, show different results. The analysis shows strong intra-month transitions - both for increase and decrease, successfully captured by the proposed AVI-BoT technique.
6. It is noteworthy that AVI-BoT prediction for 9th November 2019 (Table 2 (l), moderate to high probability) for left bank of the neck of the lake, is just 6 days before the first actual ground reporting of the outbreak dated 16th November 2019¹². Further, upper left bank (which can be

Sambhar Lake (India)



Klamath National Wildlife Refuge (U.S.A.)

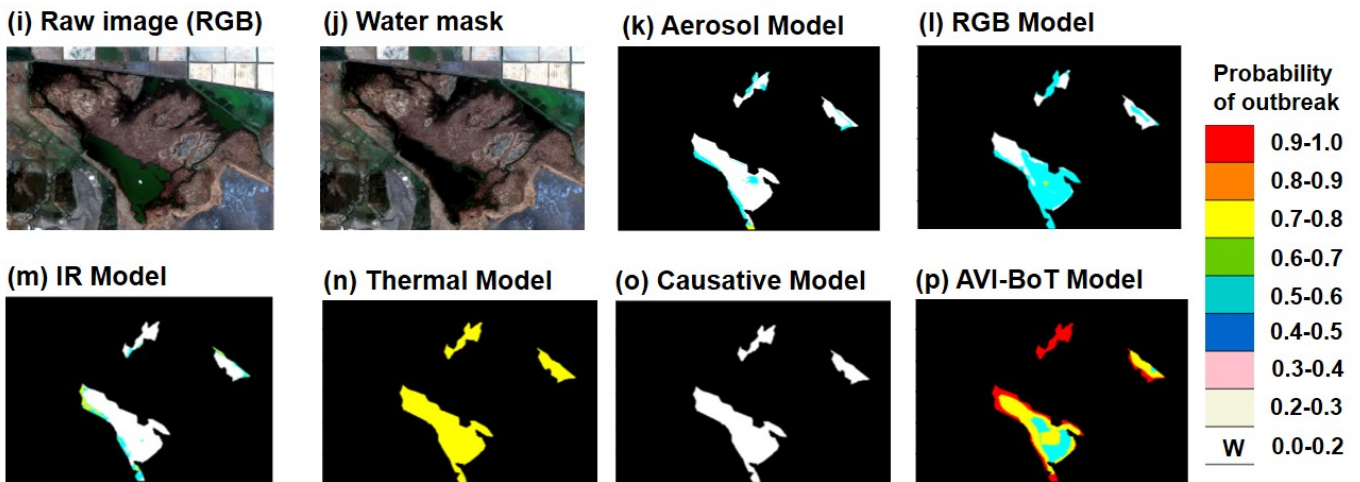


Figure 3: Prediction results on Sambhar Lake, India for 19th November 2019 ((a)-(h)) and Klamath National Wildlife Refuge, U.S.A. for 9th October 2020 ((i)-(p)).

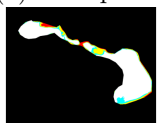
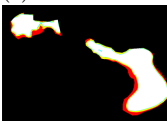
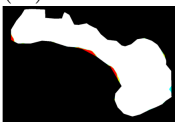
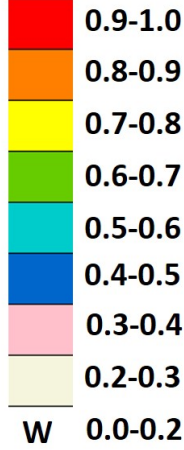
considered Nagaur area) shows moderate outbreak probability, which is in consonance with bird carcasses being reported from that area from 15th November onwards (Fig. 4).

2.2.2 Case Study 2: Klamath National Park

Klamath National Wildlife Refuge (U.S.A.) witnessed an outbreak in October 2020⁵. Causative Factors based model is unable to predict an outbreak (Fig. 3 (o)), while AVI-BoT model predicts the outbreak with fine-scale granularity (Fig. 3 (p)). Another important point to note in Fig. 3 is that the AVI-BoT model always predicts higher possibility of outbreak at the shoreline than at the center of the water body. This is in conformity with¹⁷ stating that Avian botulism is a water's edge disease, meaning that rarely are sick avi-fauna found away from the vegetation at the edge of the water or the original water's edge. For further analysis, we generated all year-round prediction maps using the proposed AVI-BoT model for 2019 shown in Table 3. To our surprise, the AVI-BoT generated prediction maps were in strong alignment not only with the expected theoretical factors behind the outbreak but also on-ground reporting of sudden outbreak increases. Some key observations from this case study are:

1. The winter months (December-February) are marked by low prevalence of Avian botulism outbreaks. (Table 3-(a), (b), (l))
2. As temperature begins to increase, the conditions turn conducive for the bacteria to develop, as evident from the increase in area with (probability > 0.9) between March-May 2019. (Table 3 (c),

Table 2: Temporal prediction maps for Sambhar Lake, India for 2017-19 using the proposed AVI-BoT model.

AVI-BoT generated Prediction Map	(a) 20 Sep 2017 	(b) 10 Oct 2017* 	(c) 27 Sep 2018 	(d) 10 Oct 2018 	(e) 25 Oct 2018 
AVI-BoT Predicted Outbreak Probability	Moderate-High	Moderate	Low	Moderate	Moderate-High
Possible hypothesis, qualitative analysis	Deficient rain may have lead to increased conditions	Moderate conditions owing to disappearance of lake	Higher than normal rain yields no evidence for existence of conditions	Conditions begin to build	Water level reduces, high probability near neck of lake
AVI-BoT generated Prediction Map	(f) 9 Nov 2018 	(g) 29 Nov 2018 	(h) 31 Aug 2019 	(i) 10 Sep 2019 	(j) 5 Oct 2019 
AVI-BoT Predicted Outbreak Probability	Moderate-High	Low-Moderate	Low	Low	Low
Possible hypothesis, qualitative analysis	Water recedes considerably, possibly due to high temp.	Water reduces further, however becomes less severe	No evidence for conditions existing	Onset of very slight conditions at lower right bank end	Slight conditions over upper left bank shoreline
AVI-BoT generated Prediction Map	(k) 25 Oct 2019 	(l) 9 Nov 2019 	(m) 19 Nov 2019 	(n) 4 Dec 2019 	Probability of outbreak  W 0.0-0.2
Magnified view of affected area					
AVI-BoT Predicted Outbreak Probability	Low-Moderate	Moderate	Moderate-High	Moderate	
Possible hypothesis, qualitative analysis	Moderate conditions begin to develop at left and right bank of neck and on top-left of lake	Moderate-High conditions at left bank of neck. Low-Moderate on upper left bank	Severe conditions develop over left bank entire shore-line	Severity on decline	

* Due to low water level in the left part, only right part of the lake is shown.

† Since outbreak at Sambhar Lake occurred in November 2019, we investigated the month of November for 2017 and 2018 for studying inter year behavior. Sept and Oct were considered as 2 immediately preceding months to study condition buildup effect. For 2019, we analyzed buildup for preceding five months.

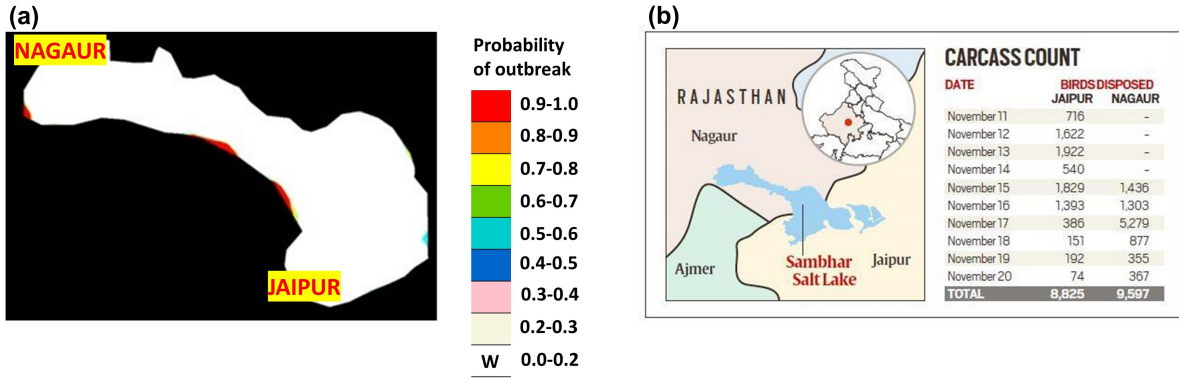


Figure 4: Confirmation of the AVI-BoT Model predictions for Sambhar Lake (India) based on comparison of: (a) Probability map generated by AVI-BoT for remote-sensing data from 19th November 2019 and (b) 9-day (i.e. Nov 11-20, 2019) ground-truth reporting for the site (Info graphic used from¹⁶).

(e))

3. During fall migration of birds (September-November), a higher probability is predicted, which is also consistent with news reporting¹⁸ (Table 3 (i)-(k)).
4. Despite reporting of water release to Lower Klamath region in beginning of September 2019¹⁹, an increase in probability of outbreak is noted from 16th August 2019 to 12th September 2019, which coincides with a reporting of sudden increase of outbreak cases¹⁸. (Table 3 (h)-(i))

Exhaustive temporal-analysis as shown in Sections 2.2.1 and 2.2.2 can help monitor contributory factors round-the-year and timely issue a pre-emptive warning, thereby helping authorities to act and save migratory birds in large numbers.

3 Discussion

The proposed AVI-BoT model outperforms the proposed literature-inspired Causative Factors model with a significantly higher accuracy. It uses Aerosol band to capture the constituents of shallow water, Visible band is the abstraction of salinity and organic matter, Infra-Red bands capture other crucial factors like pH, and Thermal bands are a direct input for temperature. Thereby, covering all relevant physical, chemical and biological parameters/features through learning fused multi-spectral satellite data.

To better understand AVI-BoT's learning of feature-space representations, we examine the progression of features learnt by AVI-BoT through successive convolution layers. These visualizations (see Fig. 5 (a)) have been generated using Klamath National Wildlife Refuge (U.S.A.) as sample inference data point for 9th October 2020. Analysis shown in Fig. 5 (a) helps us to understand the gradual progression of learning the feature space through Conv1 to Conv5 layers, and also how different feature maps contribute towards generation of the final output probability. Notably, the 15 convolution layer channels shown exhibit useful features over the entire surface of the lake. Conv1 layer output shows the network learning basic background (eg. fields) based on extracted water input shown to it. Conv2 layer shows a learning buildup over conv1 layer, that is, the network begins to learn foreground (the water body) as a whole. Conv3 layer begins to learn differentiation within lake such as edges or gradation within lake. Conv4 layer specializes in gradation and picks out specific features. The Conv5 layer shows the final composite feature which predominantly activates the network. The output prediction map column indicates the overlap area between the predominant conv5 features and the final AVI-BoT prediction map (shown in Fig. 3 (p)).

Channels (37,38,39) get activated at the edges of the lake corresponding to the high probability red zone. In channels (43,44,45), the Conv5 output shows blue over right part of lake, getting activated at moderate outbreak probability. Channels (49,50,51) correspond to the upper part of lake near the neck showing a light green haze. Thus, there exists a differentiation over water area marked by yellow in final output prediction map. Channels (55,56,57) cover lower bank and edges, however these are markedly different than the edges picked by (37,38,39). Channels (58,59,60) get activated at the right bank, marked by cyan in final output prediction map.

Table 3: Prediction maps for Klamath National Wildlife Refuge, U.S.A. for 2019 using proposed AVI-BoT model.

AVI-BoT generated Prediction Map	(a) 13 Jan	(b) 19 Feb	(c) 14 Mar	(d) 18 Apr	(e) 10 May	(f) 12 Jun	Probability of outbreak 
AVI-BoT Predicted Outbreak Probability	Low	Low	Moderate	Moderate-High	High	High	
Temp[Max,Min](C) Rainfall(mm) ²⁰	[5.9,-4.3] 92.7	[1.0,-8.1] 168.4	[7.6,-4.9] 55.4	[12.5,-0.1] 95.0	[16.8,2.1] 57.4	[22.6,4.4] 7.4	
Possible hypothesis, qualitative analysis	Low temp. and high rain possibly means unfavourable conditions	Low temp. and high rain possibly means unfavourable conditions	Temp. begins to rise, with less inflow of fresh water, conditions may become favourable	Temp. further increases	High temp. with moderate rain; No cases reported	Conditions improve compared to May	
AVI-BoT generated Prediction Map	(g) 19 Jul	(h) 16 Aug	(i) 12 Sep	(j) 22 Oct	(k) 11 Nov	(l) 24 Dec	
AVI-BoT Predicted Outbreak Probability	Moderate	Low-Moderate	Moderate-High	Moderate-High	Moderate	Low	
Temp[Max,Min](C) Rainfall(mm) ²⁰	[26.1,7.0] 1.0	[27.3,8.2] 18.5	[19.2,3.4] 64.5	[13.0,-2.8] 22.9	[11.1,-2.6] 26.9	[3.8,-4.5] 82.8	
Possible hypothesis, qualitative analysis	Area with yellow prediction (high probability pixels decrease)	Increased rain may have eased conditions by fresh water inflow	Temp. still in high range. High number of cases reported ¹⁸	Easing temp. eases conditions, however high probability on edges	Similar temp. and rain data compared to Oct. possibly leads to a similar prediction-map	Low temp. and sufficient fresh inflow of water possibly eased the situation	

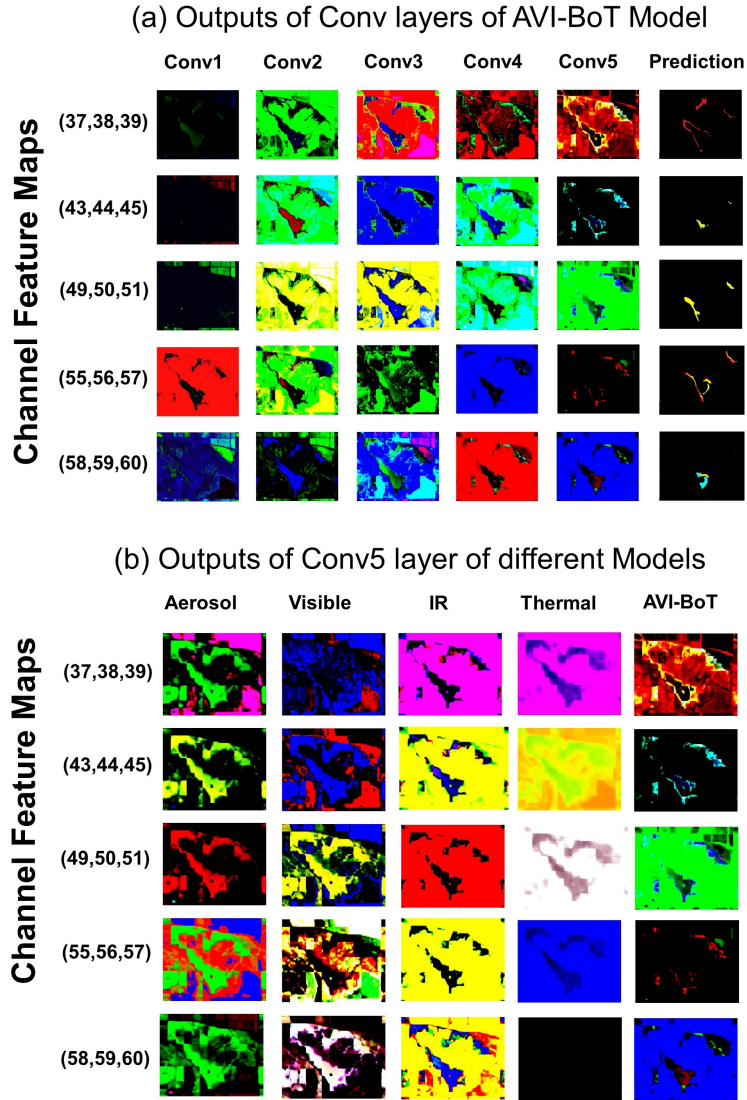


Figure 5: Illustration of progress of the feature-space learning through the convolutional layers, by proposed AI models, on Klamath National Wildlife Refuge (U.S.A.) sample input data (i.e. 10-band fused image dated 9th October 2020). Since convolutional layers have multiple channels, three successive channels are stacked in each row (viewed in false RGB) as a visual aid for human interpretation. (a) Conv. layers 1-5 using AVI-BoT model. (b) Conv. layer 5 using five different AI models.

To further examine the learnt feature space, we delve into a deeper feature analysis and additionally train four direct spectral models ((i) Aerosol, (ii) Visible (3-bands), (iii) IR (3-bands), (iv) Thermal (3-bands)). We compare the features learnt by each of the direct spectral models and try to interpret/hypothesize their contribution in the learnt feature space of AVI-BoT. The following observations can be drawn from Fig. 5 (b):

1. The activation observed at the shore of the lake is dependent on both aerosol and IR (37,38,39).
2. (43,44,45) shows a slight variation in both Aerosol and IR features, possibly contributing to the features learnt by AVI-BoT.
3. Temperature seems to have dominant role in the shallow region like upper region of the bigger water body (49,50,51).
4. (58,59,60) shows no activation by thermal input, whereas Aerosol and Visible maps show blanket activation. The differentiation learnt by AVI-BoT is possibly learnt from IR bands.

5. The activation in the interior of the lake is possibly governed by interpolation of Thermal, Aerosol and IR band.
6. The almost uniform prediction of Aerosol can be a reason of its poor performance when compared to other models despite capturing water constituents well.
7. Visible band does not seem to learn any specific feature, however performs moderately as compared to other models. Since Avian botulism is a shore line disease¹⁷, the centre of the lake is expected to yield a negative prediction and this may be the reason behind this model's lower loss.
8. IR band is seen to learn distinguishing features in it's feature map which helps the model classify it as a 'no outbreak' - (43,44,45) and (58,59,60).
9. The thermal feature map shows a sweeping output for the lake, owing to near similar temperatures taken over the surface of the lake, possibly owing to its low spatial resolution (100 m/1000 m) as well as actual temperature conditions.

Fig. 6 shows the accuracy and loss plots for training and validation for the four direct models. All models far lag behind the AVI-BoT model, with IR model being the second best in performance. This is also validated by the IR column in Fig. 5 (b) contributing the highest influence in activating the network to yield a prediction.

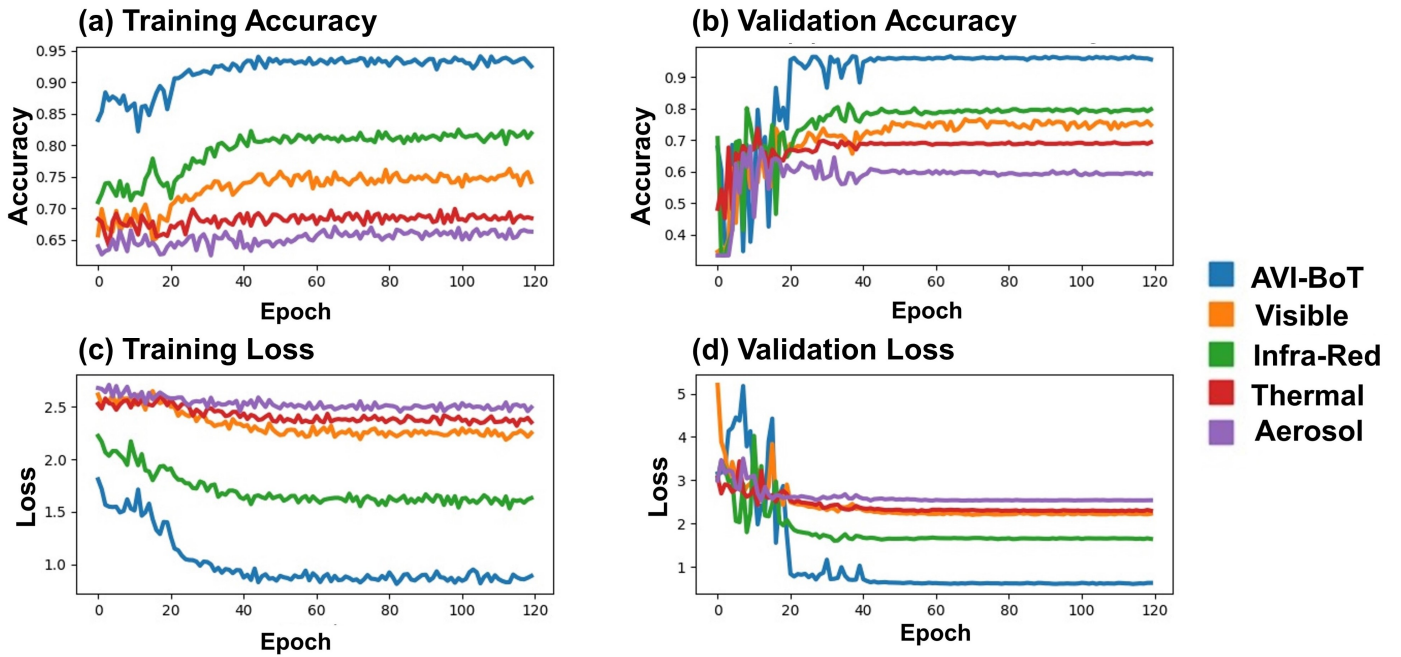


Figure 6: Epoch-wise scores for various spectral feature input representations: (a) Training Accuracy, (b) Validation Accuracy, (c) Training Loss, and (d) Validation Loss.

In Fig. 3, 3 (c) Aerosol model and 3 (d) RGB Model predict moderate conditions over the entire surface of the lake, however that is expected as it can be the result of a biased prediction relying solely on the water texture (aerosol) or optical features (visible). Similar results by 3 (f) thermal bands show their high susceptibility to slight variations, and that it is just one of the factors leading to Avian botulism, thus a model solely reliant on temperature will not be the optimal solution. 3 (e) IR model yields moderate results over the shoreline, which even though a correct prediction, does not fully capture the severity of the situation. AVI-BoT gives an accurate picture by capturing the severity as well as the spatial extent. Model outputs in Fig. 3 show that each of 3 (k) - 3 (n) predictions captures some probability of existence of conditions. However, in a scenario as grave as Klamath National Wildlife Refuge for the said dates⁵, with massive number of bird deaths, a model prediction like that shown in 3 (p) truly indicates the extent and severity of the issue at hand.

4 Conclusions

This interdisciplinary study presents the intersection of - wildlife conservation, satellite based remote-sensing technology and advanced computational techniques driven by deep learning. We build a *Bird-Area Water Bodies* Dataset (BAWD) of multi-spectral satellite images of bird-habitats covering 17 topographically diverse global locations over the period 2016-2020, with ground-truth labels backed by on-ground reportings confirming the outbreak occurrence. We further present AVI-BoT, an intelligent AI model with training accuracy of 0.94 and validation accuracy of 0.96, to forecast Avian botulism outbreaks, using open-source remote sensing data. We also validate our technique on recently reported complex Avian botulism outbreaks in Sambhar Lake (India, November 2019) and Klamath National Wildlife Refuge (U.S.A., October 2020) and confirm a highly probable prediction by our model for an outbreak. Further, temporal analysis for the two said locations using the proposed model leads to fine grain spatio-temporal decision output that is closely aligned with actual on-ground clinical diagnosis based reports. We also train five additional models (Causative Factors based and four direct spectral models) to compare and examine the evolution of the multi-spectral feature space. Proposed predictive methodology provides an efficient and scalable first-of-its-kind monitoring technique which can be used to pre-emptively protect the migratory fauna and interdependent food webs, thus contributing towards the United Nations' SDGs (Sustainable Development Goals) 13 and 14²¹.

5 Methods

5.1 *Bird-Area Water-Bodies* Dataset (BAWD)

A multi-spectral spatio-temporal dataset spanning across 17 topographically diverse global locations (15 training and 2 test) comprising a total of 659 satellite images (632 training and 27 test images) of water bodies (rivers, lakes, ponds and wetlands) which are bird habitats, was built and manually annotated for this study (see Fig. 7). Fig. 7 (c) shows the spatial variability of the dataset. The images have been generated from Sentinel EO browser²². Among the 10 bands, 7 bands are raw spectral bands taken from Sentinel 2A after L2A processing. L2A processing takes as input L1C processed image which is radio-metrically and geometrically corrected (including orthorectification and spatial registration) and performs atmospheric corrections²³. The remaining 3 bands are thermal bands which have been taken from Landsat 8 or Sentinel 3. Sentinel-3 data was used wherever Landsat-8 data was cloudy or not available for dates of interest. About $\sim 21\%$ of the total data (135 images) came from Sentinel-3. Landsat 8 is preferred for thermal maps owing to its superior spatial resolution over Sentinel 3.

For building a robust model capable of predicting Avian botulism outbreak near/in water-bodies across seasonal variability, we collected positive and negative data spanning over a time-period of ~ 3 years. Positive-labels denote conditions for Avian botulism exist while negative-labels denote non-existent botulism conditions. Positive labels were created on the basis of confirmed ground reports for the outbreak at any of the sites ([25]-[34]). The temporal spread of each positive label was adjusted over a span of two months (one month before and after) with respect to the ground reporting date of the outbreak since the conditions do not change overnight.

For samples labelled as negative, the locations are predominantly chosen from the list of Important Bird Areas (IBA) designated by BirdLife International²⁴. In some cases, confirmed news reportings stating a corrective action taken by the local authorities are also used for negative samples. Corrective actions include draining or flooding the wetland to change the environmental conditions sufficiently to stop the production of toxin by *Clostridium botulinum*. Four complex locations which have transitioned between 'outbreak' and 'no outbreak' have also been factored in the BAWD dataset to account for complex cases. Table 4 details the locations and the dates for which the samples are collected along with ground reporting evidence for labelling the sample-type (i.e. positive or negative).

5.2 Using AI to build a Predictive Model

Deep learning has recently emerged as a very powerful and flexible technique across multiple use-cases, including but not limited to object detection, intelligent feature extraction, data fusion. It is based on learning several levels of representations, where more abstract representations are computed in terms of less abstract ones. This in turn helps to make sense of data such as images, sound, and text⁴⁵.

Deep learning for image analysis is almost synonymous with applying convolutional neural networks (CNNs)^{45;46}. The convolution operation, which forms the backbone of CNNs, learns patterns from the

Table 4: Description of Positive and Negative Samples in *Bird-Area Water Bodies* (BAWD) Training Dataset (15 out of 17 locations).

Positive Data			
Location	Period of data collection	Number of images	Reported positive in:
Bromley Oxidation Pond (New Zealand)	Dec'17 - Mar'18	10	25
Firth of Thames (New Zealand)	Dec'19 - Feb'20	111	26
Kaitaia (New Zealand)	Jan'19 - Mar'19	8	27
Western Springs (New Zealand)	Jan'18 - Feb'18	2	28
Kapiti Coast (New Zealand)	Dec'17 - Mar'18	7	29
Lake Buloke (Australia)	Jan'17 - Mar'17	6	30
Sleeping Bear Dunes (U.S.A.)	Sept'19 - Nov'19	35	31
North Canterbury (New Zealand)	Jan'18 - Apr'18	18	32
Pertobe Lake (Australia)	Jan'19 - Apr'19	15	33
Radipole Lake (United Kingdom)	Aug'19 - Sept'19	33	34
Negative Data			
Location	Period of data collection	Number of images	Reported negative in:
Firth of Thames (New Zealand)	June'17 ; June'18 - Aug'18 ; June'19 - Aug'19	83	35
Lake Balaton (Hungary)	Aug'18 - Sept'18 ; Dec'18 - Feb'19 ; July'19 - Sept'19	84	1;36
Lange Lacke (Austria)	Dec'16 - Feb'17 ; July'17-Sept'17	27	1;37
Sleeping Bear Dunes (U.S.A.)	Mar'18 ; Jan'19-Feb'19 ; Dec'19 ; Feb'20	46	38
Smith and Bybee (U.S.A.)	Feb'18 -Apr'18 ;Jan'19 - Apr'19	54	39
San Carlos Reservoir (U.S.A.)	Jan'19 - Dec'19	17	40
Radipole Lake (United Kingdom)	Jan'18 - May'18; July'18 - Dec'18	12	41
North Canterbury (New Zealand)	Jan'17-Feb'17; May'17; July'17-Aug'17; Oct'17-Dec'17	10	42
Lake Pakowki (Canada)	Apr'18-Aug'18; Oct'18-Nov'18; Apr'19-Aug'19	54	43;44

(a) Selected Positive Samples Preview



(b) Selected Negative Samples Preview



(c) Bird-Area Water-Bodies Dataset (BAWD) Geographical Spread

Training Location (Positive)

- 1 Kaitaia
- 2 Western Springs
- 3 Kapiti Coast
- 4 Lake Buloke
- 5 Lake Pertobe
- 6 Bromley Oxidation Ponds

Training Location (Negative)

- 1 Lake Balaton
- 2 Lange Lacke
- 3 Smith and Bybee
- 4 San Carlos
- 5 Lake Pakowki

Complex Training Location

- 1 Firth of Thames
- 2 Sleeping Bear Dunes
- 3 North Canterbury
- 4 Radipole Lake

Test Location

- 1 Klamath National Wildlife Refuge
- 2 Sambhar Lake



- Total dataset area : ~904 Sq. Km
- Total number of positive slices : 272
- Total number of negative slices : 387

Figure 7: *Bird-Area Water-Bodies Dataset (BAWD)* details: RGB preview of few (a) Positive and (b) Negative samples (Raw data source: Modified Copernicus Sentinel data 2016-2020 /Sentinel Hub), (c) Distribution map of 17 global locations chosen for the study.

input image while preserving the spatial characteristics present in the original image, making them highly suitable for processing structured 2D data.

CNNs can learn to extract features directly from images significantly decreasing the need for manual feature extraction. In general, a CNN is composed of tens or even hundreds of convolution layers. With every convolution layer, the complexity of the learned image feature increases. The capability of CNNs to extract features in a complex hyper-space which is difficult for humans to visualize along with the ability to handle geographically variant multi-spectral data from multiple sensors, makes deep learning models extremely useful for remote sensing applications.

5.2.1 CNN Training Methodology

Each of the 10 bands (Table 5) is merged using QGIS⁵³, and water area is extracted for each wetland manually. The merge operation is carried out such that, the lowest resolution among the constituent bands is assigned to the output merged file. As shown in Table 5, Aerosol band (B01) has lowest resolution that is 60 m and is assigned to the artificially synthesised data point. Further, water extraction can also be carried out by an automated deep-learning based segmentation network like UNet⁵⁴. Selective bands from this artificial data point serve as the input to the CNN.

Table 5: Details of spectral-bands chosen and the represented parameters to generate proposed *Bird-Area Water Bodies* dataset.

Sensor	Band	Description	Wavelength (μm)	Resolution (m)	Parameters	Dependence
S2	1	Coastal/Aerosol	0.443	60	pH level, Redox potential, Presence of microbes & Water constituents	47;48
S2	2	Blue	0.490	10	Chlorophyll concentration level, DOM, Salinity level	48;49;50
S2	3	Green	0.560	10	pH level, Chlorophyll concentration level, DOM, Salinity level	47;48;49;50
S2	4	Red	0.665	10	pH level, Chlorophyll concentration level, Redox potential	47;48;51
S2	8a	Vegetation Red Edge	0.865	20	pH level, Vegetation & Organic Matter	51
S2	11	SWIR	1.610	20	Dissolved Oxygen level, Vegetation & Organic Matter	48;47
S2	12	SWIR	2.190	20	Vegetation & Organic Matter	
L8/S3	R	Temperature*	-	100/1k	Surface temperature	52
L8/S3	G	Temperature*	-	100/1k	Surface temperature	52
L8/S3	B	Temperature*	-	100/1k	Surface temperature	52

* Causative Factors based model consists of 5 bands- algebraically calculated: (i) Salinity (ii) DOM and raw spectral bands (iii)-(v) Thermal bands

All models trained in this study use a binary classification deep CNN with AlexNet⁵⁵ as the base architecture. It comprises of 5 convolutional layers followed by 2 fully connected layers. For the purpose of training, each image in the dataset is divided into 31x31 chips. We get 1127 chips from positive images and 2982 chips from negative images in the dataset. To account for the mismatch in number of positive and negative samples, higher weight is given to false-negatives than false-positives in the loss function (shown in Eq.1).

$$W.B.C.E = -[w_1 * y_{true} \cdot \log(y_{pred}) + w_2 * (1 - y_{true}) * \log(1 - y_{pred})] \quad (1)$$

Where:

W.B.C.E: Weighted Binary Cross Entropy per pixel

y_{true} : True label for a pixel

y_{pred} : Predicted label for a pixel

w_1 : Weight assigned to positive training data

w_2 : Weight assigned to negative training data

Since the proportion of chips labelled as positive:negative is 1127 : 2982 = $\sim 3 : 7$, thus the mismatch is accounted for by assigning $w_1 = 7$ and $w_2 = 3$. Further, the chips obtained are divided into $\sim 11:2$ train : validation sets. The training parameters chosen are shown in Fig. 8.

Algorithm 1 Learning rate scheduler algorithm inspired by combination of techniques in⁵⁶.

Require: Current Epoch e_i , Max Epoch E_{max} , Base Learning Rate LR_{base} , Greatest Integer Function $[x]$

Ensure: New Learning Rate LR_{new}

if $e_i < \frac{E_{max}}{6}$ **then**

$LR_{new} = LR_{base}$

else

$LR_{new} = LR_{base} \times 10^{-[\frac{e_i}{\frac{E_{max}}{6}}]}$

end if

The output of the network is a probability value that indicates the likelihood for occurrence of Avian botulism outbreak (ranging from 0 to 1). The output probability value for a chip is assigned to the center pixel of the chip. At the time of prediction, we divide an entire image of test location into 31x31 chips with stride size 1. Thus, the entire image is scanned and each pixel is assigned a probability.

5.2.2 Causative Factors based Model

In this model, we combine the most crucial causative factors responsible for the outbreak in literature⁵⁷ i.e. salinity, temperature and dissolved organic matter (DOM). Equivalent band representations for the same are calculated as shown below:

1. Salinity⁵⁰ = $10^{0.037X+1.494}$
where $X = (Band2 - Band3)/(Band2 + Band3)$
2. DOM⁴⁹ = $0.9819X + 5.6831$
 $X = Band2/Band3$
3. Temperature = taken from thermal heat maps

Where Band2 and Band3 refer to Sentinel Bands as defined in Table 5.

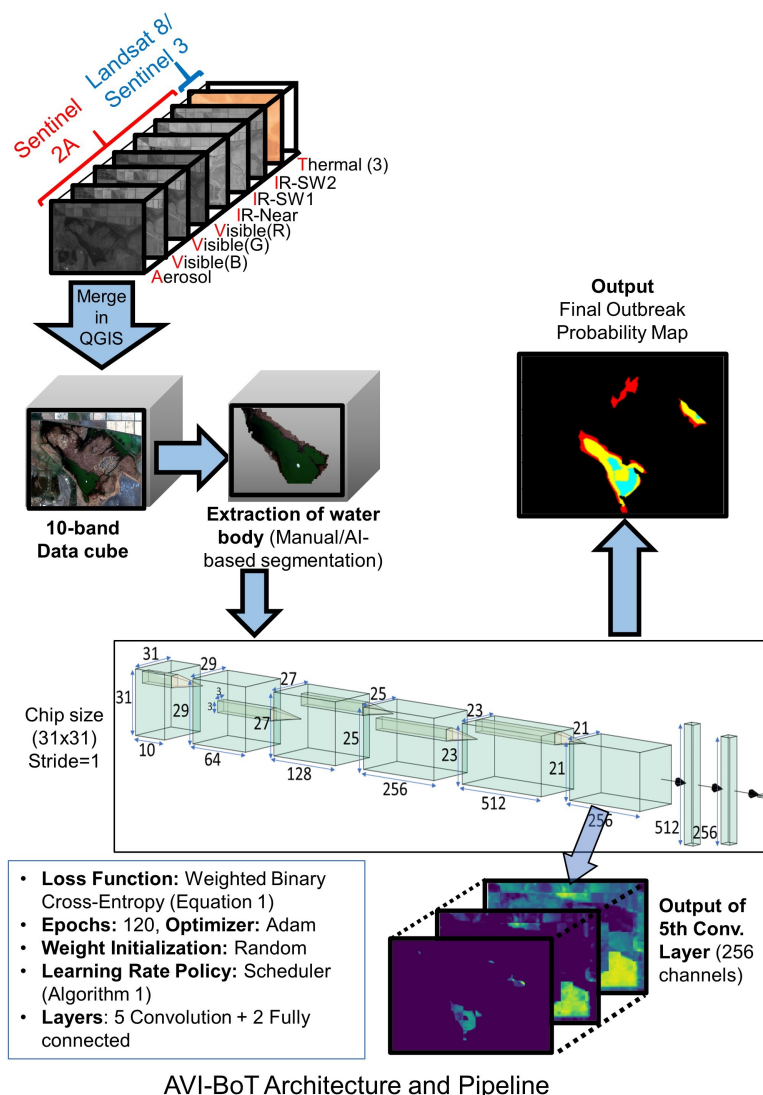


Figure 8: Proposed dataflow and deep-learning backbone used for training and inference for different networks in this study. All 10 bands are used in AVI-BoT.

5.2.3 AVI-BoT Model

Post exploration of the causative factors based model, we fuse multi-spectral bands from two different satellites to capture the impact of multiple relevant physio-chemical parameters listed in Table 5. While maintaining the tradeoff between the model size and useful features, the 10 constituent bands are carefully chosen to represent each of the wavelength bands (A,V,I,T) to remove redundancy while keeping the model size bounded. The bands - Aerosol (B01), Visible (B02-B04), NIR (B08a)-SWIR (B11,B12), Thermal (Heat maps) - capture physical, chemical and biological parameters where each of these respective ‘causative factors’ would contribute towards the decision of a potential ‘outbreak’ or ‘no-outbreak’. Fig. 8 depicts the methodology to synthesise the fused input for AVI-BoT Model and to generate a prediction on any test location.

References

- [1] Espelund, M. & Klaveness, D. Botulism outbreaks in natural environments – an update. *Frontiers in microbiology* **5**, 287 (2014).
- [2] Friend, M. & Franson, J. Field manual of wildlife diseases: General field procedures and diseases of birds. *U.S. Geological Survey* (1999). URL <https://pubs.er.usgs.gov/publication/itr19990001>.
- [3] Avian botulism – a recurring paralytic disease of wild uk waterbirds. *Veterinary Record* **185**, 261–262 (2019). URL <https://veterinaryrecord.bmj.com/content/185/9/261>. <https://veterinaryrecord.bmj.com/content/185/9/261.full.pdf>.
- [4] Anza, I. *et al.* Eutrophication and bacterial pathogens as risk factors for avian botulism outbreaks in wetlands receiving effluents from urban wastewater treatment plants. *Applied and Environmental Microbiology* **80**, 4251–4259 (2014).
- [5] Hertel, M. Avian botulism kills 40,000 birds at national wildlife refuge. *The Revelator* (2020). URL <https://therevelator.org/avian-botulism-klamath/>.
- [6] Le Gratiet, T. *et al.* Development of an innovative and quick method for the isolation of clostridium botulinum strains involved in avian botulism outbreaks. *Toxins* **12**, 42 (2020).
- [7] Rocke, T. E., Smith, S. R. & Nashold, S. W. Preliminary evaluation of a simple in vitro test for the diagnosis of type c botulism in wild birds. *Journal of wildlife diseases* **34**, 744–751 (1998).
- [8] Chellapandi, P. & Prisilla, A. Pcr-based molecular diagnosis of botulism (types c and d) outbreaks in aquatic birds. *Annals of Microbiology* **68**, 835–849 (2018).
- [9] Anniballi, F. *et al.* Management of animal botulism outbreaks: from clinical suspicion to practical countermeasures to prevent or minimize outbreaks. *Biosecurity and bioterrorism: biodefense strategy, practice, and science* **11**, S191–S199 (2013).
- [10] Woudstra, C. *Clostridium botulinum, from toxin and flagellin genotyping to Whole Genome Sequencing: An insight into the genetic diversity of human and animal botulism associated Clostridia*. Ph.D. thesis (2016).
- [11] Survey, U. G. Avian botulism. <https://www.usgs.gov/centers/nwhc/science/avian-botulism>. Accessed: 2021-01-03.
- [12] Singh, S. D. . A. Sambhar bird death: Mortality pattern indicates avian botulism, says report. *Times of India* (2019). URL <https://timesofindia.indiatimes.com/city/jaipur/sambhar-bird-death-mortality-pattern-indicates-avian-botulism-says-report/articleshow/72080003.cms>.
- [13] Hedeland, M. *et al.* Confirmation of botulism in birds and cattle by the mouse bioassay and endopep-ms. *Journal of medical microbiology* **60**, 1299–1305 (2011).
- [14] Thomas, R. Detection of clostridium botulinum types c and d toxin by elisa. *Australian Veterinary Journal* **68**, 111–113 (1991).

- [15] Le Maréchal, C. *et al.* Development and validation of a new reliable method for the diagnosis of avian botulism. *Plos one* **12**, e0169640 (2017).
- [16] Khan, H. Management, hydrology, salt pans — what’s behind rajasthan’s bird crisis? *Indian Express* (2019). URL <https://indianexpress.com/article/explained/sambhar-lake-rajasthan-bird-deaths-in-india-6129271/>.
- [17] Locke, L. N. & Friend, M. N. 13.2. 4. avian botulism: Geographic expansion of a historic disease. *Waterfowl management handbook* 3 (1989).
- [18] Current avian botulism outbreak in lower klamath basin. <https://birdallyx.net/current-avian-botulism-outbreak-in-lower-klamath-basin-heats-up/>. Accessed: 2021-01-03.
- [19] Release, K. W. U. A. P. Lower klamath lake nwr to begin receiving water from klamath project. *Klamath Falls News* (2019). URL <https://www.klamathfallsnews.org/news/lower-klamath-lake-nwr-to-begin-receiving-water-from-klamath-project>.
- [20] NOAA National Centers for Environmental information . *Climate at a Glance: County Time Series* (2020). URL <https://www.ncdc.noaa.gov/cag/>. Published November 2020, Retrieved on December 8, 2020.
- [21] Assembly, U. N. G. Transforming our world : the 2030 agenda for sustainable development, a/res/70/1. 21 October 2015. Available at: <https://www.refworld.org/docid/57b6e3e44.html> [Accessed: 2021-01-03] (2015).
- [22] Sentinel-hub. <https://apps.sentinel-hub.com/eo-browser/>. Sinergise Ltd.
- [23] Gascon, F. *et al.* Copernicus sentinel-2a calibration and products validation status. *Remote Sensing* **9**, 584 (2017).
- [24] DONALD, P. F. *et al.* Important bird and biodiversity areas (ibas): the development and characteristics of a global inventory of key sites for biodiversity. *Bird Conservation International* **29**, 177–198 (2019).
- [25] Birds die in suspected avian botulism outbreak. *Newsline, Christchurch City Council* (2018). URL <https://newsline.ccc.govt.nz/news/story/birds-die-in-suspected-avian-botulism-outbreak>.
- [26] Tantau, K. Avian botulism outbreak killing hundreds of birds around firth of thames. *Stuff* (2020). URL <https://www.stuff.co.nz/environment/119389949/avian-botulism-outbreak-killing-hundreds-of-birds-around-firth-of-thames>.
- [27] Avian botulism from sewage pond kills 600 birds. *Radio New Zealand* (2019). URL <https://www.rnz.co.nz/news/national/382315/avian-botulism-from-sewage-pond-kills-600-birds>.
- [28] Owen, C. Botulism outbreak in auckland parks killing hundreds of ducks. *stuff* (2018). URL <https://www.stuff.co.nz/environment/101002041/botulism-outbreak-in-auckland-parks-killing-hundreds-of-ducks>.
- [29] Fallon, V. Mass bird deaths at kapiti coast lake blamed on avian botulism. *Stuff* (2018). URL <https://www.stuff.co.nz/environment/101619817/mass-bird-deaths-at-kpiti-coast-lagoon-blamed-on-avian-botulism>.
- [30] Segal, Y. Cases of avian botulism found in victoria. *Agriculture Victoria* (2017). URL <https://agriculture.vic.gov.au/support-and-resources/newsletters/vetwatch-newsletter/vetwatch-october-2017/cases-of-avian-botulism-found-in-victoria>.
- [31] Travis, J. Botulism suspect behind loon deaths. *Record-Eagle* (2019). URL https://www.record-eagle.com/botulism-suspect-behind-loon-deaths/article_a9e0d01e-f1db-11e9-aa52-936af29b7971.html.
- [32] Harris, D. Outbreak kills 1000 water birds at canterbury wastewater plants. *Stuff* (2018). URL <https://www.stuff.co.nz/environment/101747128/outbreak-kills-1000-water-birds-at-canterbury-wastewater-plants>.

- [33] Creed, A. Duck mystery solved (letters to the editor). *The Standard* (2019). URL <https://www.standard.net.au/story/6394350/letters-ducks-have-gone-and-the-coots-are-not-responsible/>.
- [34] Cutler, A. Gulls across weymouth and portland found dead from disease. *Dorset Echo* (2019). URL <https://www.dorsetecho.co.uk/news/17871936.gulls-across-weymouth-portland-found-dead-disease/>.
- [35] Birdlife international (2020) important bird areas factsheet: Firth of thames. downloaded from <http://www.birdlife.org> on 04/12/2020. *BirdLife International* .
- [36] Birdlife international (2020) important bird areas factsheet: Lake balaton. downloaded from <http://www.birdlife.org> on 04/12/2020. *BirdLife International* .
- [37] Birdlife international (2020) important bird areas factsheet: Southern seewinkel and zitzmannsdorfer wiesen. downloaded from <http://www.birdlife.org> on 04/12/2020. *BirdLife International* .
- [38] Birdlife international (2020) important bird areas factsheet: Sleeping bear dunes national lakeshore mainland (including donner point to dimmick’s point and glen arbor twp beaches). downloaded from <http://www.birdlife.org> on 04/12/2020. *BirdLife International* .
- [39] Notice of a type ix decision on a proposal in your neighborhood, case file number: Lu 17-162183 cn. *City of Portland, Bureau of Development Services, Oregon Land Use Services* URL <https://www.portlandoregon.gov/bds/article/651613>.
- [40] San carlos apache tribe vs usa order. *District Court, Arizona* (2003). URL https://www.narf.org/nill/bulletins/federal/documents/san_carlos.html.
- [41] Birdlife international (2020) important bird areas factsheet: Weymouth wetlands. downloaded from <http://www.birdlife.org> on 04/12/2020. *BirdLife International* .
- [42] Birdlife international (2020) important bird areas factsheet: Canterbury (offshore). downloaded from <http://www.birdlife.org> on 04/12/2020. *BirdLife International* .
- [43] Resource, A. S. & Development. Avian botulism in alberta factsheet. *Alberta Avian Botulism Factsheet* (2004). URL <https://open.alberta.ca/dataset/4c943b95-806f-472d-a1a0-a81195e25ab3/resource/7c20e7f3-a2d6-4f76-9cc3-abbc77c74391/download/avianbotulism-factsheet-mar2004.pdf>.
- [44] Birdlife international (2020) important bird areas factsheet: Pakowki lake. downloaded from <http://www.birdlife.org> on 04/12/2020. *BirdLife International* .
- [45] LeCun, Y., Bengio, Y. & Hinton, G. Deep learning. *nature* **521**, 436–444 (2015).
- [46] LeCun, Y. *et al.* Handwritten digit recognition with a back-propagation network. In *Advances in neural information processing systems*, 396–404 (1990).
- [47] Karaoui, I. *et al.* Evaluating the potential of sentinel-2 satellite images for water quality characterization of artificial reservoirs: The bin el ouidane reservoir case study (morocco). *Meteorology Hydrology and Water Management. Research and Operational Applications* **7**, 31–39 (2019).
- [48] Pizani, F. M., Maillard, P., Ferreira, A. F. & de Amorim, C. C. Estimation of water quality in a reservoir from sentinel-2 msi and landsat-8 oli sensors. *ISPRS Annals of Photogrammetry, Remote Sensing & Spatial Information Sciences* **5** (2020).
- [49] Kutser, T. *et al.* Using satellite remote sensing to estimate the colored dissolved organic matter absorption coefficient in lakes. *Ecosystems* **8**, 709–720 (2005).
- [50] Sun, D. *et al.* Remote sensing estimation of sea surface salinity from goci measurements in the southern yellow sea. *Remote Sensing* **11**, 775 (2019).
- [51] Torres-Bejarano, F., Arteaga-Hernández, F., Rodríguez-Ibarra, D., Mejía-Ávila, D. & González-Márquez, L. Water quality assessment in a wetland complex using sentinel 2 satellite images. *International Journal of Environmental Science and Technology* 1–12 (2020).

- [52] Lafrancois, B., Riley, S., Blehert, D. & Ballmann, A. Links between type e botulism outbreaks, lake levels, and surface water temperatures in lake michigan, 1963–2008. *Journal of Great Lakes Research* **37**, 86–91 (2011).
- [53] QGIS Development Team. *QGIS Geographic Information System*. Open Source Geospatial Foundation (2009). URL <http://qgis.osgeo.org>.
- [54] Ronneberger, O., Fischer, P. & Brox, T. U-net: Convolutional networks for biomedical image segmentation. In *International Conference on Medical image computing and computer-assisted intervention*, 234–241 (Springer, 2015).
- [55] Krizhevsky, A., Sutskever, I. & Hinton, G. E. Imagenet classification with deep convolutional neural networks. *Communications of the ACM* **60**, 84–90 (2017).
- [56] Konar, J., Khandelwal, P. & Tripathi, R. Comparison of various learning rate scheduling techniques on convolutional neural network. In *2020 IEEE International Students' Conference on Electrical, Electronics and Computer Science (SCEECS)*, 1–5 (IEEE, 2020).
- [57] Rocke, T. E. & Samuel, M. D. Water and sediment characteristics associated with avian botulism outbreaks in wetlands. *The Journal of Wildlife Management* 1249–1260 (1999).

Data and Code availability

Authors can share entire BAWD dataset and code used in this study upon reasonable request.

Acknowledgements

Authors would like to acknowledge CYRAN AI Solutions for providing computing resources to perform this study. We thank Sentinel and Copernicus programs for hosting useful remote-sensing data freely in public domain.

Competing Interests

Authors would like to declare no competing interests.

Author Contributions

N.B designed the AVI-BoT and custom models. All authors worked on AI model refinement and optimization. D.M and J.S contributed to building the BAWD dataset. All authors contributed to analysis and result interpretation. N.B and M.S wrote and edited the manuscript. All authors contributed to reviews. M.S. designed the study.